Supporting Information

Tuning the sensitivity of genetically encoded fluorescent potassium indicators through structure-guided and genome mining strategies

Cristina C. Torres Cabán[1,2,3], Minghan Yang[4,5,6,7], Cuixin Lai[4,5,6], Lina Yang[4,5,6], Fedor V. Subach[8], Brian O. Smith[9], Kiryl D. Piatkevich[4,5,6]*, Edward S. Boyden[1,2,3,10,11,12,13,14]*

[1]McGovern Institute for Brain Research, MIT, Cambridge, 02139, MA, USA

[2]Department of Biological Engineering, MIT, Cambridge, 02139, MA, USA

[3]Department of Media Arts & Sciences, MIT, Cambridge, 02139, MA, USA

[4]School of Life Sciences, Westlake University, Hangzhou, 310024, Zhejiang Province, China

[5]Westlake Laboratory of Life Sciences and Biomedicine, Hangzhou, 310024, Zhejiang Province, China

[6]Institute of Basic Medical Sciences, Westlake Institute for Advanced Study, Hangzhou, 310024, Zhejiang Province, China

[7]College of Physics, Jilin University, Changchun, 130012, Jilin Province, China

[8]Complex of NBICS Technologies, National Research Center "Kurchatov Institute", Moscow, 123182, Russia

[9]Institute of Molecular, Cell & Systems Biology, College of Medical Veterinary & Life Sciences, University of Glasgow, Glasgow, G128QQ, UK

[10]Koch Institute for Integrative Cancer Research, MIT, Cambridge, 02139 MA, USA

[11]Howard Hughes Medical Institute, Chevy Chase, 20815, MD, USA

[12]Department of Brain and Cognitive Sciences, MIT, Cambridge, 02139 MA, USA

[13]K. Lisa Yang Center for Bionics, MIT, Cambridge, 02139, MA, USA

[14]Center for Neurobiological Engineering, MIT, Cambridge, 02139, MA, USA

*Correspondence to: kiryl.piatkevich@westlake.edu.cn and edboyden@mit.edu

Supporting Information

Supplementary Table 1	NMR and refinement statistics for Ec-Kbp.K^+.
Supplementary Table 2	Geometry of the K^+ binding site in Ec-Kbp.K.
Supplementary Table 3	Physical properties of the tested KRaION1 mutants and homologs under screening conditions in solution.
Supplementary Table 4	Search results obtained from protein BLAST of the Ec-Kbp sequence.
Supplementary Table 5	Binding affinity and dynamic range characterization of genetically encoded indicators made with alternative binding domains.
Supplementary Table 6	Properties of indicators measured in HeLa cells permeabilized with valinomycin.
Supplementary Table 7	Binding affinity (K_d) measurements obtained at varied conditions in vitro.
Supplementary Table 8	Primer sequences used for site-directed mutagenesis of Ec-Kbp.
Supplementary Figure 1	Selectivity of KRaION1, KRaION1/D9N, and KRaION2 to K^+.
Supplementary Figure 2	Structure of Ec-Kbp.K^+ and mutation sites.
Supplementary Figure 3	Emission spectra of mNG-Ec-Kbp and variants upon K^+ administration.
Supplementary Figure 4	Cell calibration curves for KRaION1/D9N, KRaION1, and KRaION2 under specific conditions.
Supplementary Figure 5	The experimental workflow of the perfusion system setup.

Supplementary Table 1. NMR and refinement statistics for Ec-Kbp.K^+.

	Ec-Kbp.K^+	
NMR distance and dihedral constraints		
Distance constraints		
Total NOE	5626	
Ambiguous	2741	
Unambigous	2885	
Intra-residue	1237	
Inter-residue		
Sequential ($\|i-j\|=1$)	715	
Medium-range ($\|i-j\|<4$)	371	
Long-range ($\|i-j\|>5$)	562	
CO to K^+ restraints	5	
Dihedral angle restraints[a]		
φ	81	
ψ	81	
Structure statistics		
Violations (mean and s.d.)		
Distance constraints (Å)	$4.54\times10^{-2}\pm1.93\times10^{-3}$	
Violations per structure > 0.5 Å	1.5±0.87	
Violations per structure > 0.3 Å	15±3.4	
Deviations from idealized geometry		
Bond lengths (Å)	$5.63\times10^{-3}\pm1.75\times10^{-4}$	
Bond angles (°)	$0.607\pm1.61\times10^{-2}$	
Impropers (°)	$1.61\pm8.69\times10^{-2}$	
Average pairwise r.m.s. deviation[b] (Å)	All residues	Ordered residues[c]
Heavy	1.56±0.23	0.77±0.06
Backbone	1.02±0.22	0.43±0.06
Ramachandran statistics (%)		Ordered residues[d]
Favoured		93±2
Additionally allowed		7±2
Disallowed		0±0

[a]Chemical shift based, not used in refinement. [b]Pairwise r.m.s. deviation was calculated among 20 refined structures. [c]Residues 3-14, 25-50, 54-89, 91-101, 105-149. [d]Residues 3-14, 25-148.

Supplementary Table 2. Geometry of the K^+ binding site in Ec-Kbp.K.

	Distance O_aK (Å)		**Angle O_aKO_b (°) for b[a]**								**Angle C_aO_aK (°)**	
a[a]	dO_aK[b]	±	*10*	±	*75*	±	*77*	±	*80*	±	$\angle C_aO_aK$[b]	±
7	2.69	0.0581	78	17	146	16	106	12	79	12	38.6	7.5
10	2.62	0.0239			132	8.5	66	4.3	125	6.7	76.4	3.72
75	2.64	0.0509					93	7.4	85	13	56.4	4.65
77	2.86	0.053							75	3.5	131	4.63
80	2.69	0.0409									56.1	2.03

[a]a and b indicate the amino acid residue numbers of coordinating carbonyl groups in Ec-Kbp with O and C denoting the carbonyl oxygen and carbon atoms, respectively. [b]Mean distances (d) and angles (∠) are presented with their standard deviations (±) estimated from the ensemble of 20 structures.

Supplementary Table 3. Physical properties of the tested KRaION1 mutants and homologs under screening conditions in solution.

Indicator	Absorbance (nm)[a]	Fitted K_d (mM)[b]	$\Delta F/F_{max}$ (%)[c]	Brightness relative to KRaION1 (%)[d]	Folding efficiency (%)[d]
KRaION1	406/505	12±4	222	100	100
mNG-Ec-Kbp-D9N	405/504	27± 7	449	89	68
mNG-Ec-Kbp-D9A	405/504	17±5	506	46	25
mNG-Ec-Kbp-E12A	405/504	28±7	355	90	62
mNG-Ec-Kbp-E12Q	405/504	52±15	275	58	33
mNG-Ec-Kbp-K8A	405/505	17±15	164	91	72
mNG-Pa-Kbp	405/504	5±2	233	45	259
mNG-C-Kbp	405/505	19±6	204	104	126
mNG-Hv-Kbp	405/504	68±18	94	88	38
mNG-D-Kbp	405/504	7±3	173	37	26
mNG-Ec-Kbp-A10G	405/504	n.d.[e]	n.d.[e]	50	22
mNG-Ec-Kbp-N76D	405/504	n.d.	n.d.	20	11
mNG-Ec-Kbp-I77A	405/505	n.d.	n.d.	74	42
mNG-Ec-Kbp-I77G	405/504	n.d.	n.d.	46	47
mNG-Ec-Kbp-I77S	405/504	n.d.	n.d.	59	33
mNG-Ec-Kbp-I80A	405/504	n.d.	n.d.	36	34
mNG-Ec-Kbp-I80G	405/504	n.d.	n.d.	17	40
mNG-Ec-Kbp-I80S	405/504	n.d.	n.d.	65	33
mNG-Ec-Kbp-D9K	405/504	n.d.	n.d.	71	36
mNG-Ec-Kbp-E12K	405/505	n.d.	n.d.	2	34

[a]K^+ titration was conducted in non-isotonic conditions in a range of 0 - 310 mM K^+. Equation used to fit data and obtain K_d is: $Q=(Q_{max}-Q_0)Y+Q_0$. [b]Max fluorescence dynamic range ($\Delta F/F_{max}$) values represent fluorescence change at baseline of 0 mM to the highest fluorescence value obtained within the range of 0−310 mM K^+. [c]Brightness and folding efficiency were expressed as a percentage relative to KRaION1 (*i.e.*, KRaION1 = 100%). [d]For values listed as n.d. = not determined; these indicators did not exhibit a fluorescence change response to K^+ titration.

Supplementary Table 4. Search results obtained from protein BLAST of the Ec-Kbp sequence.

Query[a]	Homolog[b]	Percent Identity (%)	Alignment Length (aa)	Number of mismatches	Gap Opens	Query Start (aa)	Query End (aa)	Sequence Start (aa)	Sequence End (aa)	E-value	Bit score	% Positives
WP_000522415.1	MNG82101.1 (C-Kbp)	72	148	41	0	1	148	1	148	3.11E-83	230	85
WP_000522415.1	NP_253865.1 (Pa-Kbp)	55	148	64	2	1	148	1	145	3.07E-58	167	74
WP_000522415.1	SUS08588.1 (D-Kbp)	53	147	63	4	1	147	1	141	1.84E-47	139	67
WP_000522415.1	VAV91021.1 (Hv-Kbp)	45	148	76	3	1	148	1	143	1.54E-38	117	61

[a]Query corresponds to the GenBank accession number of the Ec-Kbp sequence utilized for sequence alignment. [b]Accession numbers of the homologs found by the metagenomic protein BLAST search.

Supplementary Table 5. Binding affinity and dynamic range characterization of genetically encoded indicators made with alternative binding domains.

Indicator	Fitted K_d (mM)[a]	$\Delta F/F_{max}$ (%)[b]
mNG-C-Kbp	39±7	213
mNG-Pa-Kbp	48±6	262
mNG-Hv-Kbp	63±15	106
mNG-D-Kbp	112±35	147

[a]K^+ titration was conducted in isotonic conditions in a range of 0.1–700 mM K^+. Equation used to fit data and obtain K_d is: $Q=(Q_{max}-Q_0)Y+Q_0$. [b]Fluorescence dynamic range ($\Delta F/F_{max}$) values represent percent max fluorescence change within the range of 0.1–700 mM K^+.

Supplementary Table 6. Properties of indicators measured in HeLa cells permeabilized with valinomycin.

Indicator	$\Delta R/R_{max}$ (%)[a]	Fitted Kd (mM)[b]
KRaION1	219±25	23±3
KRaION2	225±28	20±2
GINKO1	255±150	3±0.23

[a]Dynamic range of excitation fluorescence ratio measured in live HeLa cells permeabilized with valinomycin within the range of 0-150 mM K^+. [b]Intracellular characterization of K_d was done in the range of 0 - 150 mM K^+. Equation used to fit data and obtain K_d is: $Q=(Q_{max}-Q_0)Y+Q_0$.

Supplementary Table 7. Binding affinity (K_d) measurements obtained at varied conditions in vitro.

	Condition 1[a]	**Condition 2[b]**
Indicator	**Fitted K_d (mM)**	**Fitted K_d (mM)**
KRaION1	69±10	42±10
KRaION1/D9N	138±21	100±6
KRaION2	96±9	66±9
mNG-C-Kbp	39±7	34±5
mNG-Pa-Kbp	48±6	42±14
mNG-Hv-Kbp	63±15	133±22[c]
mNG-D-Kbp	112±35	22±14
GINKO1	17±7	21±10

[a]K^+ titration was conducted in isotonic conditions in a range of 0.1 – 700 mM K^+. [b]K^+ titration was conducted at constant 5 mM Na^+ with an increasing concentration of 0.1 – 250 mM K^+. [c]K^+ titration was conducted at 5 mM Na^+ with an increasing concentration of 0.1–650 mM K^+ for indicator to reach a binding plateau. Equation used to fit all data in this table to obtain K_d is: $Q=(Q_{max}-Q_0)Y+Q_0$.

Supplementary Table 8. Primer sequences used for site-directed mutagenesis of Ec-Kbp.

Mutant[a]	Primer Sequence 5'- 3'
Ec-Kbp-Fw-K8A	CGG CCT GTT CAA CTT CGT GGC CGA CGC CGG CGA GAA GC
Ec-Kbp-Rv-K8A	GCT TCT CGC CGG CGT CGG CCA CGA AGT TGA ACA GGC CG
Ec-Kbp-Fw-D9N	CGG CCT GTT CAA CTT CGT GAA GAA CGC CGG CGA GAA GCT GTG
Ec-Kbp-Rv-D9N	CAC AGC TTC TCG CCG GCG TTC TTC ACG AAG TTG AAC AGG CCG
Ec-Kbp-Fw-D9K	CGG CCT GTT CAA CTT CGT GAA GAA GGC CGG CGA GAA GCT GTG
Ec-Kbp-Rv-D9K	CAC AGC TTC TCG CCG GCC TTC TTC ACG AAG TTG AAC AGG CCG
Ec-Kbp-Fw-D9A	CGG CCT GTT CAA CTT CGT GAA GGC CGC CGG CGA GAA GCT GTG
Ec-Kbp-Rv-D9A	CAC AGC TTC TCG CCG GCG GCC TTC ACG AAG TTG AAC AGG CCG
Ec-Kbp-Fw-E12K	CGT GAA GGA CGC CGG CAA GAA GCT GTG GGA TGC CGT G
Ec-Kbp-Rv-E12K	CAC GGC ATC CCA CAG CTT CTT GCC GGC GTC CTT CAC G
Ec-Kbp-Fw-E12A	CGT GAA GGA CGC CGG CGC CAA GCT GTG GGA TGC CGT G
Ec-Kbp-Rv-E12A	CAC GGC ATC CCA CAG CTT GGC GCC GGC GTC CTT CAC G
Ec-Kbp-Fw-E12Q	CGT GAA GGA CGC CGG CCA GAA GCT GTG GGA TGC CGT G
Ec-Kbp-Rv-E12Q	CAC GGC ATC CCA CAG CTT CTG GCC GGC GTC CTT CAC G
Ec-Kbp-Fw-A10G	GGC CTG TTC AAC TTC GTG AAG GAC GGC GGC GAG AAG CTG TGG GAT GC
Ec-Kbp-Rv-A10G	GCA TCC CAC AGC TTC TCG CCG CCG TCC TTC ACG AAG TTG AAC AGG CC
Ec-Kbp-Fw-N76D	CTG GTG GCC GTG GGC GAC ATC AGC GGA ATC GCC AGC
Ec-Kbp-Rv-N76D	GCT GGC GAT TCC GCT GAT GTC GCC CAC GGC CAC CAG
Ec-Kbp-Fw-I80A	CGT GGG CAA CAT CAG CGG AGC CGC CAG CGT GGA CGA TCA AG
Ec-Kbp-Rv-I80A	CTT GAT CGT CCA CGC TGG CGG CTC CGC TGA TGT TGC CCA CG
Ec-Kbp-Fw-I80G	CGT GGG CAA CAT CAG CGG AGG CGC CAG CGT GGA CGA TCA AG
Ec-Kbp-Rv-I80G	CTT GAT CGT CCA CGC TGG CGC CTC CGC TGA TGT TGC CCA CG
Ec-Kbp-Fw-I80S	CGT GGG CAA CAT CAG CGG AAG CGC CAG CGT GGA CGA TCA AG
Ec-Kbp-Rv-I80S	CTT GAT CGT CCA CGC TGG CGC TTC CGC TGA TGT TGC CCA CG
Ec-Kbp-Fw-I77A	GGT GGC CGT GGG CAA CGC CAG CGG AAT CGC CAG CG
Ec-Kbp-Rv-I77A	CGC TGG CGA TTC CGC TGG CGT TGC CCA CGG CCA CC
Ec-Kbp-Fw-I77G	GGT GGC CGT GGG CAA CGG CAG CGG AAT CGC CAG CG
Ec-Kbp-Rv-I77G	CGC TGG CGA TTC CGC TGC CGT TGC CCA CGG CCA CC
Ec-Kbp-Fw-I77S	GGT GGC CGT GGG CAA CAG CAG CGG AAT CGC CAG CG
Ec-Kbp-Rv-I77S	CGC TGG CGA TTC CGC TGC TGT TGC CCA CGG CCA CC

[a]Each mutant has a forward (Fw) and reverse (Rv) primer sequence.

Supplementary Figure 1. Selectivity of KRaION1, KRaION1/D9N, and KRaION2 to K^+.

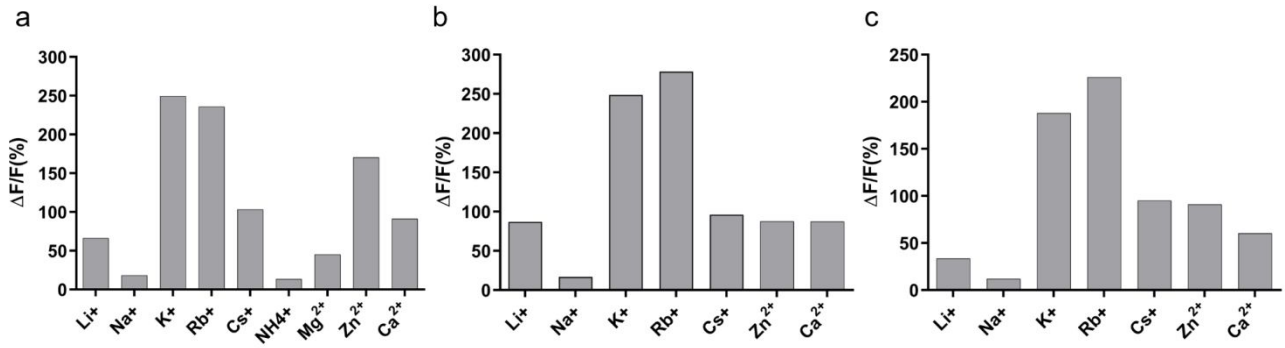

(a) Calculated maximum fluorescence change (ΔF/F %) of KRaION1 to K^+ and other cations obtained by titration of Li^+, Na^+, Rb^+, Cs^+, NH_4^+, Mg^{2+}, and Ca^{2+} in the range 0 - 260 mM, and Zn^{2+} in the range 0 - 260 μM. (b) Calculated maximum fluorescence change (ΔF/F %) of KRaION1/D9N to K^+ and other cations obtained by titration of Li^+, Na^+, Rb^+, Cs^+, and Ca^{2+} in the range 0 - 260 mM, and Zn^{2+} in the range 0 - 260 μM. (c) Calculated maximum fluorescence change (ΔF/F %) of KRaION2 to K^+ and other cations obtained by titration of Li^+, Na^+, Rb^+, Cs^+, and Ca^{2+} in the range 0 - 260 mM, and Zn^{2+} in the range 0 - 260 μM.

Supplementary Figure 2. Structure of Ec-Kbp.K^+ and mutation sites.

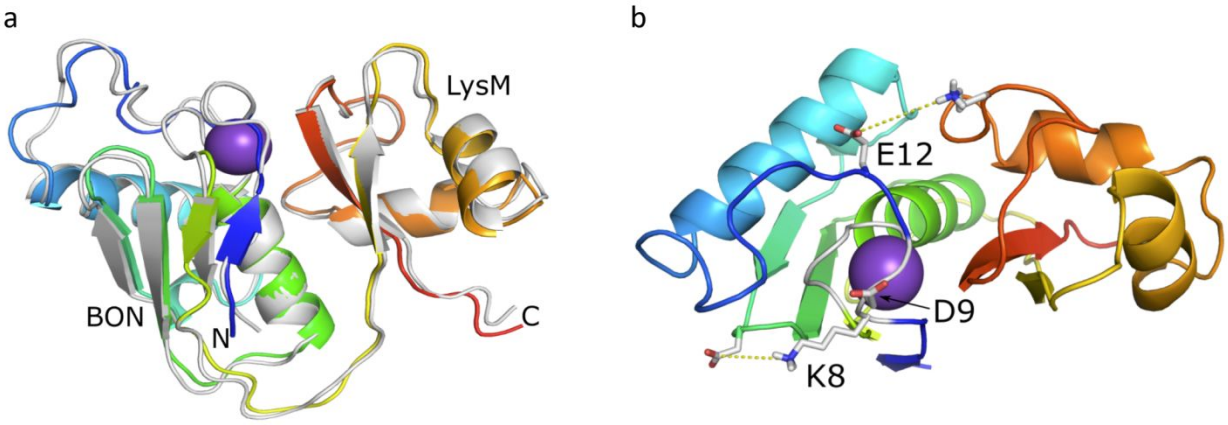

(a) Refined structure of Ec-Kbp in its potassium bound state, shown as the rainbow-colored cartoon, is overlaid with the previously calculated structure of Ec-Kbp (PDB:5FIM) in grey. The potassium ion is represented by a purple sphere. (b) Location of the K8, D9, and E12 residues (shown as sticks) that were chosen for mutation in respect to the potassium binding site. The potassium ion is represented by a purple sphere and the protein backbone shown in cartoon representation coloured from blue at the N-terminus through to red at the C-terminus. Residues D52 and K133, which may make ionic interactions with K8 and E12, respectively, are also shown in stick form with yellow dashed lines connecting them.

Supplementary Figure 3. Emission spectra of KRaION1 and variants upon K^+ administration.

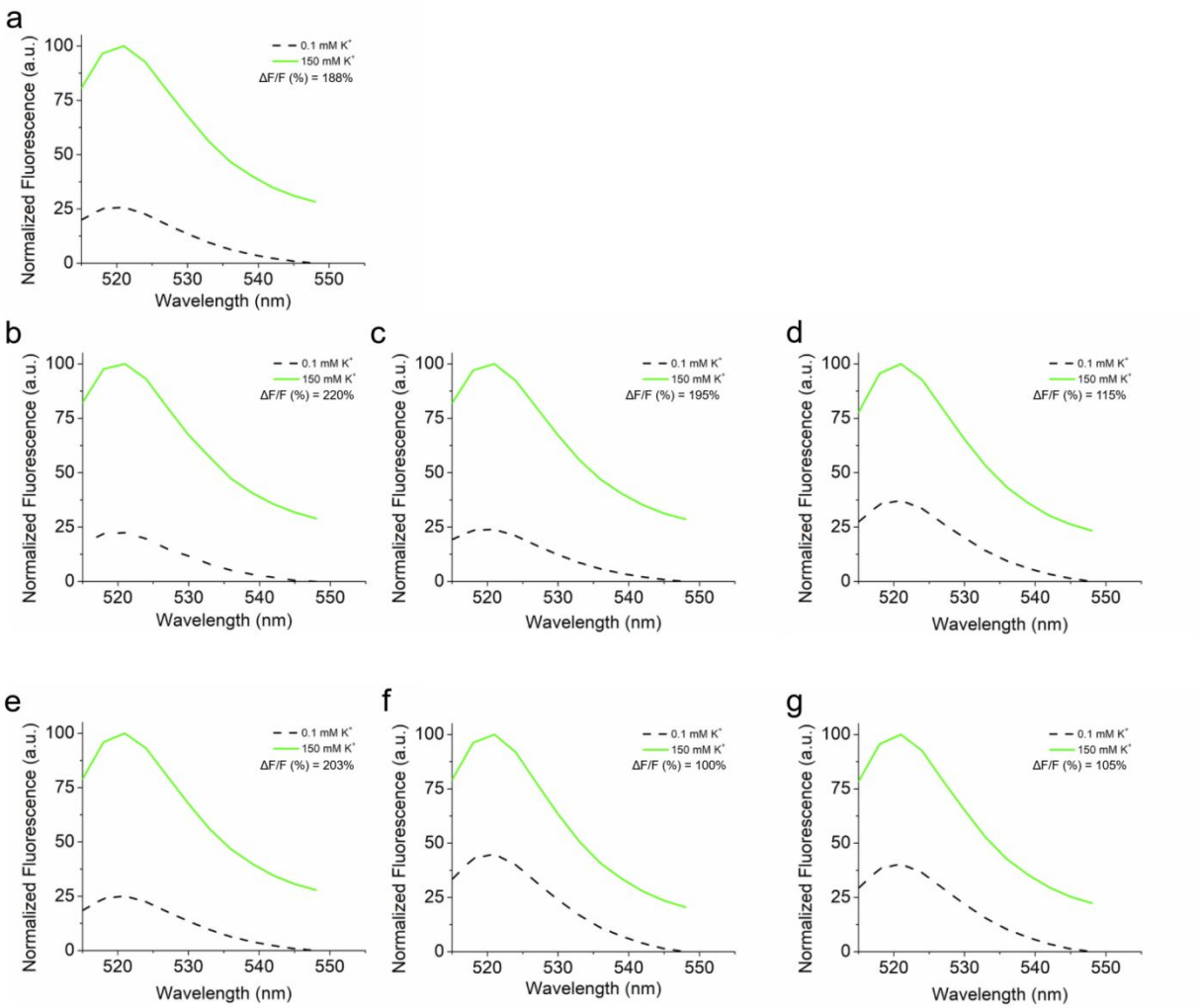

(a, b, c, d, e, f, g) Fluorescence emission spectra of KRaION1, KRaION1/D9N, KRaION2, mNG-C-Kbp, mNG-Pa-Kbp, mNG-Hv-Kbp, and mNG-D-Kbp, respectively, at 0.1 mM and 150 mM potassium at pH = 7.3. $\Delta F/F_{max}$ refers to the maximum fluorescent change observed when measured in the concentration range of 0.1 - 700 mM K^+.

Supplementary Figure 4. Cell calibration curves for KRaION1/D9N, KRaION1, and KRaION2 under specific conditions.

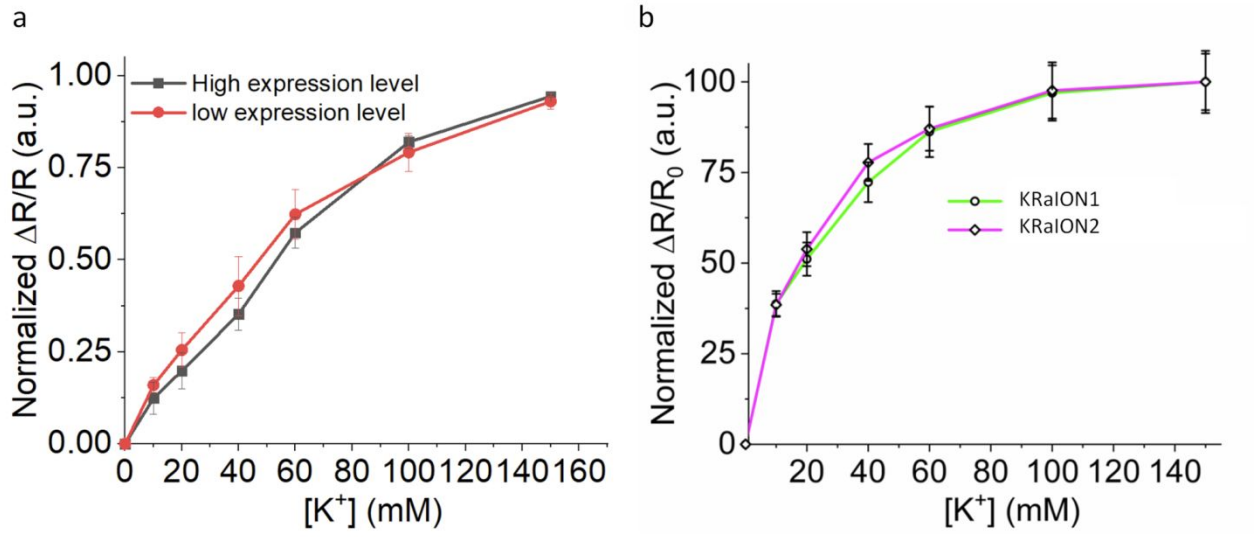

(a) Binding titration curves for cells equilibrated with valinomycin and CCCP with high and low expression of KRaION1/D9N presented as normalized excitation ratio F_{478nm}/F_{390nm} (n=2 cells for high expressors and n=11 from low expressors from 1 FOV; data points, mean, and error bars, standard deviation). (b) Binding titration curves for KRaION1 and KRaION2 when equilibrated with valinomycin presented as normalized excitation ratio F_{478nm}/F_{390nm} (n=16 and 26 cells from 3 independent transfections for KRaION1 and KRaION2, respectively; data points, mean, error bars, standard deviation).

Supplementary Figure 5. The experimental workflow of the perfusion system setup.